3D channel simulations including scattering from non-gaussian rough surfaces

Yann Cocheril, Rodolphe Vauzelle, Lilian Aveneau
SIC Laboratory, University of Poitiers, Blvd Marie et Pierre Curie, BP 30179, 86962 Futuroscope Chasseneuil Cedex, France
cocheril@sic.univ-poitiers.fr

***Abstract*— An original approach to characterize radio channel in indoor environments composed of rough surfaces is presented. It is based on algorithms developed for the image rendering field that are extended to the radio wave propagation. To simulate rough surfaces scattering, these algorithms need information about roughness. A possible solution consists of quantifying roughness by using statistical distributions of surface parameters, such as heights, slopes and local normals. In this paper, different theoretical statistical laws are presented and a fitting is realized with corresponding distributions of three real samples of wall roughcasts. For these cases, the best parameter to quantify the roughness is presented. Next, two algorithms which take roughness into account are detailed and compared with first results of channel simulations in indoor environments at 60 GHz.**

Index Terms—*3D ray tracing, indoor environments, Monte Carlo methods, rough surfaces scattering.*

I. INTRODUCTION

NOWADAYS, an increasing interest is devoted to wide-band applications like wireless local area networks. Because the present multimedia services are more and more demanding in terms of high bit rate and thus large bandwidth, the working frequency increases. In order to deploy such wireless systems we have to study the radio channel.

Ray tracing (RT) techniques [1] are widely used in radio communications to predict the channel behaviour. Indeed, they are fast and applicable as long as the wavelength is smaller than the dimensions of objects which interact during the wave propagation. RT is based on the geometrical optics (GO) [2] extended with the (geometrical) uniform theory of diffraction (GTD/UTD) [3,4]. RT techniques take into account several physical mechanisms with a great accuracy.

For example, the single direction of a reflected wave from a smooth surface is given by Snell-Descartes's reflection law, and its power is computed by Fresnel reflection coefficients [2]. However, if we consider millimetric systems, a surface can be considered slightly rough (wavelength measures 5 mm at 60 GHz). From such a surface, the reflection direction is not only the specular one. Indeed, some fraction of the energy is scattered in others directions, due to the roughness of the surface [5-8].

This paper presents the study of three real man made rough surfaces like wall roughcasts in order to include scattering phenomenon in channel simulations. To avoid memory consuming and huge computational time we prefer to describe them statistically. In Section II, for each sample of roughcasts, we test different statistical distributions for several roughness parameters such as heights, slopes and local normals. The theoretical tested laws are: gaussian [9], ex-gaussian [10], or Edgeworth series [11]. In Section III, we explain how the choice of a roughness parameter according to a statistical law influences scattered waves from rough surfaces. Next, to include scattering phenomenon in a full 3D ray tracing [12], we can use two different methods related to computer graphics [13],which are explained in Section IV. This section, also presents first results of the influence of rough surfaces in a channel simulation. Indeed, we show impulse responses (IR), mean delays and delay spreads results. They allow a comparison between both integrated methods in smooth and rough indoor environments. We compare these results with classical full 3D ray tracing ones obtained in smooth indoor environments.

II. ROUGH SURFACES

A. Definition

Two different ways are generally used to describe a rough surface. From real rough surfaces, we can store in a structure called *height map* all heights of the surface (also called *height field*). This technique may be deployed, thanks to a laser sensor [14]. However, this technique has some drawbacks like the memory consuming and the long acquisition time. A second method consists in describing rough surfaces using few roughness parameters according to appropriate statistical laws. The drawback of this method is that we have to choose the roughness parameters and statistical laws to have an accurate

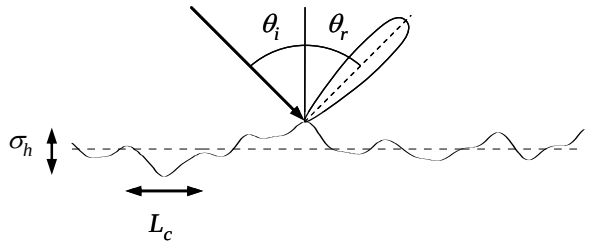

Fig. 1. Profile of a rough surface with its parameters σ_h (standard deviation) and L_c (correlation length).

description of the rough surface.

The Rayleigh criterion (1) is widely used to know whether a surface is rough or not (Fig. 1). It respects the following principle: a surface can be considered smooth if the phase difference between two rays reflected by two different heights on the surface is smaller than $\pi/2$ in the far field [7].

$$\sigma_h < \frac{\lambda}{8\sin\theta_i} \tag{1}$$

B. Theoretical laws

We present in the following the theoretical laws that were chosen to test the fit of distributions of the deterministic rough surfaces (Fig. 2) parameters such as heights *h*, slopes *s* and local normals α. All formulas are taken for heights parameters, but are applicable to slopes and local normals too.

1) Gaussian distribution:

Generally, the scattering problem on rough surfaces is solved with the Kirchhoff Approximation [5,7] (KA), the Small Perturbation Method [6] (SPM), or the Small Slope Approximation [8] (SSA). These three methods are validated for gaussian rough surfaces. "Gaussian" means the height distribution $p_G(h)$ of the rough surface corresponds to a normal law, with a null average m_h and a standard deviation σ_h:

$$p_G(h) = \frac{1}{\sqrt{2\pi}\sigma_h} e^{-\frac{1}{2}\left(\frac{h}{\sigma_h}\right)^2} \tag{2}$$

It is also related to the fact that autocorrelation function $\phi_{hh'}(l)$ is gaussian:

$$\phi_{hh'}(l) = e^{-\left(\frac{l}{L_c}\right)^2} \tag{3}$$

The autocorrelation function gives the correlation between two heights *h*, *h'*, separated by a distance *l*.

These two assumptions lead to a normal distribution for the slopes $p_s(s)$ [6,7,9] of the rough surfaces with a null average m_s and a standard deviation σ_s verifying:

$$\sigma_s^2 = -\sigma_h^2 \times \phi''_{hh'}(0) = \frac{2\sigma_h^2}{L_c} \tag{4}$$

We can also apply the gaussian hypothesis directly to slopes and local normals of the rough surface.

2) Ex-Gaussian distribution:

This distribution is produced by the convolution of normal and exponential distributions [10]. The Ex-Gaussian function $p_{EG}(h)$ (5) has three parameters: *m*, σ and τ.

$$p_{EG}(h) \approx \frac{1}{2\tau} e^{\left(\frac{m-h}{\tau}+\frac{\sigma^2}{2\tau^2}\right)}\left[1+erf\left(\frac{h-m}{\sigma}-\frac{\sigma}{\tau}\right)\right] \tag{5}$$

These parameters have a simple relationship (6) with the three first central moments $\mu_{1,2,3}$:

$$\begin{aligned} \mu_1 &= m+\tau \\ \mu_2 &= \sigma^2+\tau^2 \\ \mu_3 &= 2\tau^3 \end{aligned} \tag{6}$$

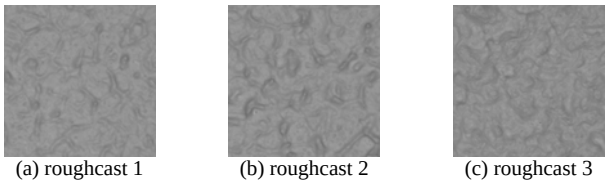

(a) roughcast 1 (b) roughcast 2 (c) roughcast 3

Fig. 2. Roughcast samples (2 cm square) with an increase roughness level from left to right.

The skewness property γ_3 (7) is taken into account with this distribution.

$$\gamma_3 = \frac{\mu_3}{\mu_2^{3/2}} \tag{7}$$

3) Edgeworth Series (ES):

It is an asymptotic expansion of the Gaussian distribution [11]. This latter is multiplied by polynomials corresponding to the successive terms in Edgeworth series. These terms have a direct relationship with central moments, so we can include the skewness γ_3 (7), the kurtosis γ_4 (12), and much others properties in this distribution. Let the standard normal distribution be:

$$\varphi(f) = \frac{1}{\sqrt{2\pi}} e^{-\frac{f^2}{2}}, \text{ with } f = \frac{h-m_h}{\sigma_h} \tag{8}$$

The asymptotic expression of the Gaussian distribution $p_{ES3}(h)$ of order 3 (in terms of central moments) is:

$$p_{ES3}(h) = \varphi(f)\left[1+\frac{\gamma_3}{6}H_3(f)\right] \tag{9}$$

Note that the skewness is taken into account. To include the kurtosis, we have to use asymptotic expression of order 4:

$$p_{ES4}(h) = \varphi(f)\psi(f) \tag{10}$$

with

$$\begin{aligned} \psi(f) &= 1+\frac{\gamma_3}{6}H_3(f)+\frac{\gamma_4-3}{24}H_4(f)+\frac{\gamma_3^2}{72}H_6(f) \\ H_3(f) &= f^3-3f \\ H_4(f) &= f^4-6f^2+3 \\ H_6(f) &= f^6-15f^4+45f^2-15 \end{aligned} \tag{11}$$

The expression of the kurtosis is:

$$\gamma_4 = \frac{\mu_4}{\mu_2^{4/2}} \tag{12}$$

C. Deterministic and statistical distributions comparisons

Now, we study the fitting between deterministic and theoretical statistical distributions for roughness parameters which are respectively heights, slopes and local normals.

1) Heights distributions:

For example, Fig. 3 shows fitting results obtained for the four statistical laws (2), (5), (9), (10) presented in Section II.B. We can observe (Fig. 3.a) that the widely accepted Gaussian hypothesis for the heights is not much accurate. Others studied distributions (Fig. 3.b, Fig. 3.c and Fig. 3.d) fit better the deterministic one than the Gaussian model.

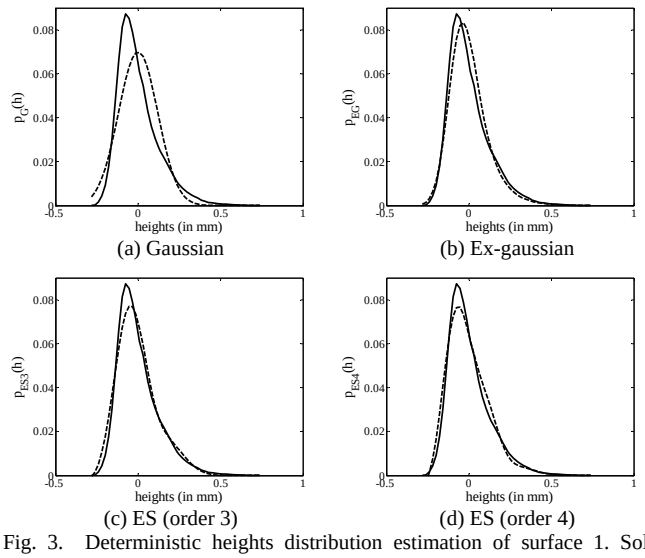

(a) Gaussian (b) Ex-gaussian

(c) ES (order 3) (d) ES (order 4)

Fig. 3. Deterministic heights distribution estimation of surface 1. Solid curves are deterministic distribution while dashed curves are statistical ones.

To quantify their quality we have to use a criterion. We use the well known Kolmogorov-Smirnov (KS) criterion [15] which computes the maximum probability error between two distributions. We present in Table I the KS test results for each theoretical laws and rough surfaces.

The fitting between deterministic and statistical distributions is improved by using higher order moments rather than the two first ones (m_h and σ_h). Indeed, the KS test results significantly decrease when we use Ex-Gaussian or Edgeworth series. In the following, the heights distribution used is an Edgeworth series with a 4th decomposition order.

2) Slopes distributions:

The same study was realized on the slopes distributions of the three rough surfaces in two orthogonal directions (x and y). The corresponding KS test results are presented in Table I.

TABLE I
KOLMOGOROV-SMIRNOV RESULTS : MAXIMUM ERROR PROBABILITY (%)

Surface	Direction	Gaussian	Ex-gaussian	ES (order 3)	ES (order 4)
Heights Distributions:					
1		9.75	4.56	3.45	2.87
2		5.24	5.05	2.99	4.12
3		3.81	3.01	1.87	1.10
Slopes Distributions:					
1	x	4.24	5.46	4.17	4.03
	y	4.60	4.69	4.74	3.95
2	x	6.21	5.99	6.71	22.73
	y	7.06	7.17	8.60	26.70
3	x	3.81	3.84	3.91	11.62
	y	3.64	3.60	3.64	11.04
Local Normals Distributions:					
1	x	2.06	1.79	1.86	1.19
	y	2.70	2.55	2.57	1.72
2	x	2.36	4.03	2.09	1.38
	y	3.04	-	3.01	1.66
3	x	0.66	0.57	0.52	0.24
	y	0.66	0.50	0.56	0.26

x and y are two orthogonal directions in the rough surface.

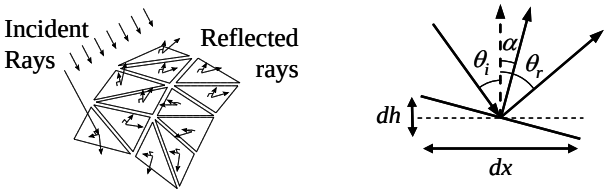

(a). Global (b). Local (2D)

Fig. 4. Reflection process on a rough surface.

There is a significant difference with the results obtained for heights distributions. Indeed errors are quietly constant between the tested distributions. So, the simplest Gaussian model can be chosen to model slopes.

3) Local normals distributions:

Table I presents the KS test results for local normals distributions estimation. In comparison with slopes ones, all errors decrease. Edgeworth series (order 4) give the best fitting results. This model is used in the following to model local normals.

III. INFLUENCE ON SCATTERING

Best statistical laws are now identified for each roughness parameter. In order to include the more realistic scattering phenomenon in channel simulations, we have to choose the best laws in terms of field distributions results.

A. Field distributions

To compute the scattering field from a rough surface, we use a method similar to KA [5,7]. We decompose the deterministic rough surface in micro-facets [16] (Fig. 4.a). Each one receives a part of the emitted power and reflects it in its own specular direction. Thus, heights distribution gives the phase variations in the far-field, while slopes and local normals ones give the reflected directions.

In a particular direction, the scattering power is weighted by the probability to have a well directed micro-facet (cf. Fig. 4.b). Thus, a statistical expression of the scattering field in a particular direction θ_r, with n contributions is derived:

$$E^r_{//,\perp}(\theta_r) = R_{//,\perp}(\theta_r) \times E^i_{//} \times e^{-j(\Phi_i+\Phi_r)} \times \frac{1}{N}\sum_{k=1}^{n} e^{-j\varphi_k} \quad (13)$$

with : . $E^r_{//,\perp}(\theta_r)$: Reflected field in direction θ_r,

. $R_{//,\perp}(\theta_r)$: Fresnel reflection coefficient in direction θ_r,

. $\Phi_i + \Phi_r$: Total phase due to free-space propagation,

. φ_k : Phase shift due to the height of the k^{th} micro-facet (follows heights distribution),

. n : Number of well directed micro-facets in θ_r direction (follows reflected directions distribution (16)),

. N : Total number of micro-facets.

According to (14), slopes distribution (15) becomes (16).

$$p_a(a)|da| = p_b(b)|db| \text{ and } \alpha = \frac{\theta_i + \theta_r}{2} \quad (14)$$

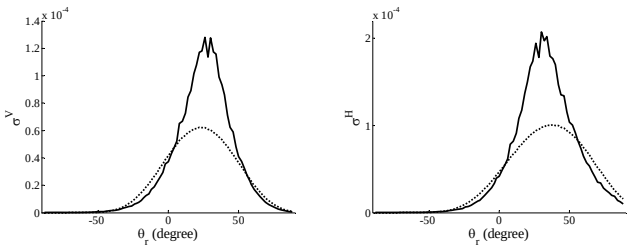

(a) RPDF computation using slopes

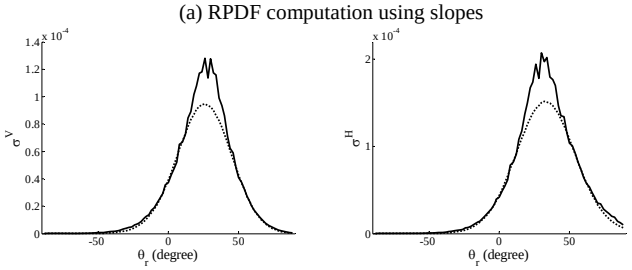

(b) RPDF computation using local normals

Fig. 5. RPDF for roughcast number 1 in vertical (σ^V) and horizontal (σ^H) polarizations, with an incident angle equal to -30°. Solid curves are RPDF computed from height maps while dashed curves are obtained statistically.

$$p_s(s) = \frac{1}{\sqrt{2\pi}\sigma_s} e^{-\frac{1}{2}\left(\frac{s}{\sigma_s}\right)^2} \tag{15}$$

$$p_{\theta_r}(\theta_r) = \frac{1}{2\sqrt{2\pi}\sigma_s \cos^2\left(\frac{\theta_i+\theta_r}{2}\right)} e^{-\frac{1}{2}\left(\frac{\tan\left(\frac{\theta_i+\theta_r}{2}\right)}{\sigma_s}\right)^2} \tag{16}$$

In the same way, according to (10) and (14), local normals distribution (17) becomes (18).

$$p_\alpha(\alpha) = \frac{1}{\sqrt{2\pi}\sigma_\alpha} e^{-\frac{1}{2}\left(\frac{\alpha}{\sigma_\alpha}\right)^2} \psi\left(\frac{\alpha}{\sigma_\alpha}\right) \tag{17}$$

$$p_{\theta_r}(\theta_r) = \frac{1}{2\sqrt{2\pi}\sigma_\alpha} e^{-\frac{1}{2}\left(\frac{\theta_i+\theta_r}{2\sigma_\alpha}\right)^2} \psi\left(\frac{\theta_i+\theta_r}{2\sigma_\alpha}\right) \tag{18}$$

B. Reflected power density functions (RPDF)

Applying the previous principle, we compute RPDF from a rough profile using (13), in vertical and horizontal polarizations (respectively σ^V and σ^H). For example, results for roughcast 1 (cf. Fig. 2.a) are presented in Fig. 5. Fig. 5.a and Fig. 5.b respectively show RPDF results computed using slopes and local normals distributions.

Clearly, it appears that the use of local normals distributions gives better agreement between deterministic and statistical RPDF results. Indeed, KS test errors for local normals estimation are smaller than the slopes ones (Table I). To conclude, we can say that our three samples of roughcasts are best described using a 4th order Edgeworth series on local normals.

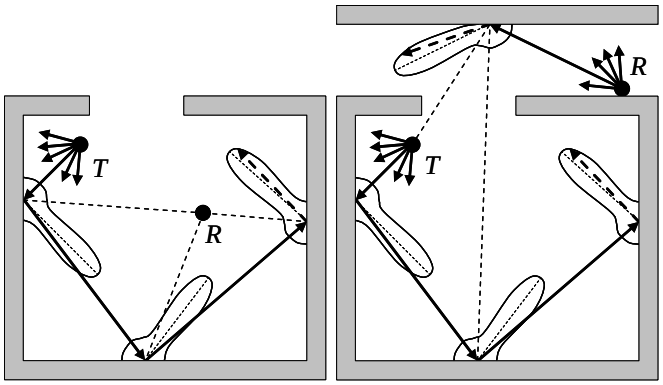

(a) Path Tracing (PT) (b) Bi-Directional PT

Fig. 6. Principles of Path Tracing and Bi-Directional Path Tracing for three allowed reflections.

IV. WAVE PROPAGATION ALGORITHMS AND SIMULATIONS

To include rough surface scattering in channel simulations, we have to use others methods than classical ray tracing techniques. In the following, we describe two valuable techniques based on Monte Carlo methods [13] which are able to sample RPDF simulating scattering from rough surfaces. These two methods are compared in details in [17].

A. Path Tracing (PT)

The principle of PT [18] is similar to ray launching. Many rays are uniformly sent from the transmitter T and propagated in the environment. When a ray impinges on a rough surface, it is reflected in a random direction, according to the statistical parameters of the hit surface. Moreover, if a Line-Of-Sight (LOS) exists between the hit point and the receiver R, a second ray is sent to this latter, with a magnitude weighted by the probability to have a well directed micro-facet. The process goes on recursively until a fixed number of interactions. Fig. 6.a shows an example of wave propagation in a room for three allowed reflections.

B. Bi-Directional Path Tracing (BDPT)

The previous method has a major drawback. Indeed, if LOS does not exist between hit points and the receiver, no energy is received. To eliminate this drawback, we use a bi-directional method. It consists of two parallel PT which interact between themselves [19]. For example, for two emitted rays from both antennas (Fig. 6.b), we search all existing LOS between their hit points. If a LOS is found, a ray has a probability to pass through it with a certain probability due to the roughness

TABLE II
MEAN DELAY AND DELAY SPREAD MEASUREMENTS:
RESULTS ARE EXPRESSED IN NANO SECONDS

	Path Tracing		Bi-Directional	
	τ_m (in ns)	D_s (in ns)	τ_m (in ns)	D_s (in ns)
Smooth Surfaces	11.3	14.1	13.9	14.0
Surface 1	5.0	11.0	8.1	12.4
Surface 2	4.5	10.4	7.1	11.8
Surface 3	3.7	9.3	6.0	11.0

τ_m means mean delay while D_s means delays spread.

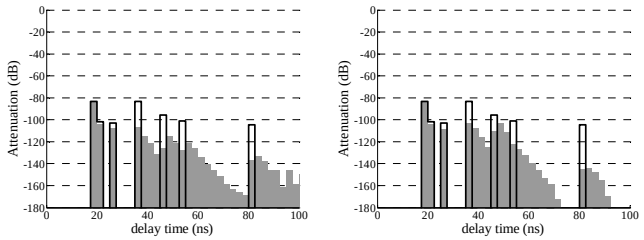

(a) PT (b) Bi-Directional PT

Fig. 7. IR obtained for a 10m square room composed with roughcast number 1 (2 reflections, f=60 GHz). Empty bars are IR obtained with a classical ray tracing while the full ones are IR obtained with our two methods.

parameters. In other words, when a ray is reflected from a hit point to another one, its magnitude is weighted with the probability to have a reflection in this direction.

C. Simulation Results

Both previous algorithms have been implemented in a full 3D ray tracing software [12]. They allow to compute Impulse Responses (IR) and their corresponding mean delay τ_m and delay spread D_s in rough indoor environments. Roughness is integrated using a 4th order ES of the local normals. So standard deviation, skewness and kurtosis are used.

First results of simulations can be obtained with 10x10x2.5 meters square room without inside obstacles (Fig. 6.a). Its walls are composed with smooth and rough surfaces presented in Fig. 2. For example, Fig. 7 shows two impulse responses for roughcast 1. Results for others rough surfaces are presented in terms of mean delay and delay spread in Table II.

We can observe that some paths are obtained in smooth case and that a dispersion of their energy in new ones is due to the roughness. This principle makes the impulse response to be more continuous. This particular behavior is confirmed by channel measurements [20]. Table II shows that mean delay and delay spread decrease when the level roughness increases.

V. CONCLUSIONS AND FUTURE WORKS

A method is presented to characterize roughness properties. We study three samples of real wall roughcasts. We show that the widely accept Gaussian hypothesis from man made rough surfaces is not accurate, and then proposed to use higher order moments. For example 4th Edgeworth series decomposition well estimates heights and local normals distributions. On the contrary, slopes ones are well modeled with Gaussian laws.

Next, we have presented how to compute the scattering field using statistical distributions of reflected directions. They are computed from slopes or local normals ones. A small difference of accuracy between different models influences significantly the reflected power densities results. For the studied roughcasts samples, local normals distributions are retained instead of slopes distributions.

Finally, first results of impulse responses for path tracing and bi-directional path tracing in a single real scene with different levels or roughness are presented. Bidirectional method presents a faster attenuation like path tracing.

In future, a complete study using numerous and various indoor environments has to be performed. It will allow us to compare the influence of material properties in addition to roughness level. Furthermore convergence and performance of both algorithms will be compared. Finally, we have to confront our results with measurements to validate these methods in channel simulations field.

ACKNOWLEDGMENT

We thank C. Bourlier, a CNRS researcher at laboratory IREENA of Nantes University (France), for his help, advises, and knowledge in rough surfaces scattering field.

REFERENCES

[1] G. A. Deschamps, "Ray techniques in electromagnetics," *Proc. IEEE*, vol. 60, no 9, pp. 1022–1035, Sept. 1972.

[2] C. A. Balanis, *Advanced Engineering Electromagnetics.* New York: John Wiley and Sons, 1989.

[3] J. B. Keller, "Geometrical theory of Diffraction," *J. Opt. Soc. Amer.*, vol. 52, no. 2, pp. 116–130, Feb. 1962.

[4] R. G. Kouyoumjian and P. H. Pathak, "A uniform geometrical theory of diffraction for an edge in a perfectly conducting surface," *Proc. IEEE*, vol. 62, no 11, pp. 1448–1461, Nov. 1974.

[5] J. A. Oglivy, *Theory of wave scattering from random rough surfaces*, Hilger, 1991.

[6] F. T. Ulaby, R. K. Moore and A. K. Fung, *Microwave remote sensing: active and passive*, vol. 2, Addison-Wesley, 1982.

[7] P. Beckmann and A. Spizzichino, *The scattering of electromagnetic waves from rough surfaces*, Pergamon, 1963.

[8] A. G. Voronovich, *Wave scattering from rough surfaces*, 2nd ed., Germany: Springer series on Wave Phenomena, 1999.

[9] D. Didascalou, M. Döttling, N. Geng and W. Wiesbeck, "An approach to include stochastic rough surface scattering into a deterministic ray-optical wave propagation modelling," *IEEE Trans. Antennas Propagat.*, vol. 51, no. 7, pp. 1508–1515, Jul. 2003.

[10] A. Heathcote, "RTSYS: A DOS application for the analysis of reaction time data," *Behavior Research Methods, Instruments, & Computers*, vol. 28, no. 3, pp. 427–445, 1996.

[11] M. S. Longuet-Higgins, "The effect of non-linearities on statistical distributions in the theory of sea waves," *J. Fluid Mech.*, vol. 17, pp. 459–480, 1963.

[12] F. Escarieu, Y. Pousset, R. Vauzelle and L. Aveneau, "Outdoor and indoor characterization by a 3D simulation software," *IEEE PIRMC'2001*, San Diego, Oct. 2001.

[13] P. Shirley, "Physically based lighting calculations for computer graphics," Ph.D Thesis, University of Illinois, Nov. 1990.

[14] H. Zahouani, R. Vargiolu, M. T. Do, "Characterization of microtexture related to wet road/tire friction," *AIPRC/PIARC*, Jun. 2000.

[15] I. M. Chakravarti, R. G. Laha and J. Roy, *Handbook of methods of applied statistics*, vol. 1, John Wiley and Sons, 1967.

[16] D.T. Lee and B. J. Schacter, "Two algorithms for constructing a Delaunay triangulation," Int. J. Conput. Inf. Sci., vol. 3, no. 9, pp. 219-242.

[17] Y. Cocheril, R. Vauzelle, L. Aveneau, "Comparison between two original methods including scattering in 3D channel simulations," *ECWT'06*, Manchester, England, Sept. 2006.

[18] E. P. Lafortune, "Mathematical models and Monte Carlo algorithms for physically based rendering," Ph.D Thesis, University of Leuven, Feb. 1996.

[19] E. P. Lafortune and Y. D. Willems, "Bi-Directional path tracing," *Compugraphics'93*, Alvor, Portugual, pp. 145–153, Dec. 1993.

[20] T. Zwick, T. J. Beukema and H. Nam, "Wideband Channel Sounder With Measurements and model for the 60 GHz Indoor Radio Channel," *IEEE Trans. Veh. Technol.*, vol. 54, no. 4, pp. 1266–1277, Jul. 2005.